B-spline-based multichannel *K*-matrix method for atomic photoionization

T. K. Fang

Institute of Atomic and Molecular Sciences, Academia Sinica, P.O. Box 23-166, Taipei, Taiwan 10764, Republic of China

T. N. Chang

Department of Physics and Astronomy, University of Southern California, Los Angeles, California 90089-0484

We present a *B*-spline-based multichannel *K*-matrix method following an extension from a *B*-spline-based configuration-interaction approach. Theoretical procedures are presented in detail for its application to photoionization from two-electron and divalent (e.g., alkaline-earth) atoms. Numerical examples, including doubly excited photoionization spectra above the $N=2$ threshold from the He $1s2s$ ^1S metastable state, are also given.

I. INTRODUCTION

Using a *B*-spline-based configuration-interaction (BSCI) approach for a single continuum [1,2], Chang and co-workers examined in detail the effects of mutlielectron interactions on strongly energy-dependent doubly excited photoionization spectra from ground and bound excited states of a number of two-electron and light divalent (e.g., alkaline-earth) atoms [3,4]. The purpose of this paper is to present an extension of the BSCI approach for a single continuum to a *B*-spline-based multichannel *K*-matrix (BSK) approach for multiple continua. Explicit theoretical procedures for applications to photoionization from two-electron or divalent atoms are given in detail. Similar to the BSCI approach, the radial part of the basis functions in the BSK approach is also set to *zero* at the boundary (i.e., at $r=R$) to retain the simplicity in the computational algorithm enjoyed by the BSCI approach.

The basic theoretical procedures of the BSK approach closely follow the *K*-matrix methods detailed earlier by Starace [5] and Moccia and co-workers [6]. In essence, for a particular ionization channel γ, its corresponding *incoming-wave-normalized* channel wave function $\Psi_{\gamma E}$ is expressed as a linear combination of eigenchannels [similar to Eq. (4.54) of Ref. [5]]. Parallel to all other multichannel theoretical approaches, the eigenchannel, designated by a channel index Γ at a total energy E, is given as a linear combination of a judiciously chosen open-channel wave function $|\Phi_{\gamma_o E}\rangle$, which represents the *individaul open channel*, i.e.,

$$|\Gamma E\rangle = \sum_{\gamma_o} |\Phi_{\gamma_o E}\rangle U_{\gamma_o \Gamma}(E)\cos\eta_\Gamma(E), \qquad (1)$$

where $U_{\gamma_o\Gamma}(E)$ is an orthogonal transformation matrix at an energy E, and the eigenphase shift η_Γ represents the interactions between $|\Phi_{\gamma_o E}\rangle$. The eigenphase shift η_Γ and the matrix $U_{\gamma_o\Gamma}(E)$ are obtained by diagonalizing the *on-the-energy-shell K* matrix, which will be discussed in detail in Sec. II. Similar to the *normal modes* for a complex system,

the *eigenchannels* are intimately related to the dynamics of the atomic process, although they do not in general represent directly the atomic states.

In Sec. II, we present explicitly the theoretical procedures which extend the single channel BSCI approach to the *B*-spline-based multichannel *K*-matrix approach. Although attempts are made to minimize the formulas that are already presented elsewhere in other *K* matrix works, some equations are included at times to ensure that a precise and consistent theoretical procedure is presented. The *K* matrix is evaluated numerically using a *discretization* procedure similar to the one employed by Moccia and co-workers [6]. Detailed computational procedures are presented in Sec. III. In Sec. IV, we demonstrate the effectiveness of the BSK method by its applications to the photoionization from the ground state of He and H⁻. Also presented are the doubly excited resonance spectra above the $N=2$ threshold following the photoionization from He $1s2s$ ^1S metastable state.

II. THEORETICAL PROCEDURES

A. Discretized basis set

Similar to the BSCI approach, the basis set employed in the BSK approach consists of a number of two-electron *configuration series* $n_i l_i l$ [1,2]. Each $n_i l_i l$ series includes a set of two-electron configurations corresponding to one of the electrons in a fixed *inner* orbital $n_i l_i$ and an outer electron with orbital angular momentm l but variable energy (both negative and positive) over an entire set of eigenfuntions $\chi_{\nu l}$ of a one-particle radial equation

$$h_l^{eff}(r)\chi_{\nu l}(r) = \varepsilon_{\nu l}\chi_{\nu l}(r), \qquad (2)$$

where h_l^{eff} is an effective one-particle radial Hamiltonian. For a two-electron atom, h_l^{eff} represents a simple hydrogenic Hamiltonian. For alkaline-earth atoms, the *frozen-core Hartree-Fock* (FCHF) Hamiltonian (including the model potentials) detailed in Ref. [2] remains to be our choice. Following the same numerical procedures employed in the BSCI approach, the radial function $\chi_{\nu l}$ is expanded in terms of a set of B splines $B_i(r)$ of total number N_l confined between $r=0$ and $r=R$, i.e.,

$$\chi(r) = \sum_i C_i B_i(r). \qquad (3)$$

The boundary conditions that $\chi(r=0)=\chi(r=R)=0$ leads to a total of N_l-2 *discretized* basis functions for each $n_i l_i l$ configuration series. For a *closed channel*, we have already learned from our BSCI calculations that such a choice is particularly effective for a numerical computation.

For an *open ionization channel*, a choice of radial functions which closely represent the outgoing ionized electron may lead to a more precise physical interpretation of the atomic process. In the BSK approach, first, we denote each open channel γ_o by a configuration series $n_o l_o l$ which corresponds to an outgoing l electron leaving the inner electron in a $n_o l_o$ orbital of the residual ion. The hydrogenic and FCHF orbitals remain our choice as the one-particle radial function for the *inner* $n_o l_o$ electron. For the one-particle radial function representing the outer electron, we follow the BSCI procedure by diagonalizing the Hamiltonian matrix of the total nonrelativistic Hamiltonian H, constructed from a basis including *only* a single $n_o l_o l$ configuration series. The outer electron, now denoted by μl, will then be represented by a one-particle function defined by Eq. (50) of Ref. [2], i.e.,

$$\xi_{\mu l}(r) = \sum_{\nu}^{N_l-2} C^{\mu}_{n_o l_o, \nu l} \chi_{\nu l}(r), \qquad (4)$$

where $C^{\mu}_{n_o l_o, \nu l}$ represents an eigenvector corresponding to a new orbital μl. This new orbital is equivalent to the one-particle orbital generated by Eq. (10) in Ref. [7], where we have already demonstrated that it more effectively represents the orbital of the outer electron in an open channel.

Symbolically, the *discretized* basis set in the BSK approach corresponding to a configuration series can be expressed as

$$|\gamma\mu\rangle \equiv \begin{cases} \sum_{\nu} C^{\mu}_{n_o l_o, \nu l} |n_o l_o, \nu l\rangle & \text{(open channel)} \\ |n_c l_c, \mu l\rangle & \text{(closed channel)}, \end{cases} \qquad (5)$$

where γ is the channel index. In other words, for an open channel, the basis is constructed from the product of $\chi_{n_o l_o}$ and $\xi_{\mu l}$ and for a closed channel the product of $\chi_{n_c l_c}$ and $\chi_{\mu l}$. The basis are orthogonal between any two configuration series, i.e.,

$$\langle \gamma'\mu' | \gamma\mu \rangle = \delta_{\gamma'\gamma} \delta_{\mu'\mu}. \qquad (6)$$

In addition, the basis functions corresponding to *open channel* also satisfy an addition condition

$$\langle \gamma_o'\mu' | H | \gamma_o\mu \rangle = \delta_{\gamma_o'\gamma_o} \delta_{\mu'\mu} \varepsilon_{\gamma_o\mu}. \qquad (7)$$

Asymptotically, at large r, the radial function $\xi_{\mu l}$, corresponding to an outgoing l electron in an open channel γ with a linear momentum $k_\mu = k$ and an energy $\varepsilon_\mu = k^2 = \varepsilon$, is given by

$$\xi_{\varepsilon l}(r) \xrightarrow[r \to R]{} A \sin\left(k - \frac{\pi l}{2} + \frac{q \ln(2kr)}{k} + \sigma_l^C + \delta_\gamma\right), \qquad (8)$$

where q is the effective nuclear charge experienced by the outgoing electron, σ_l^C is the Coulomb phase shift, and δ_γ is the scattering phase shift due to the short-range interaction. The amplitude A approaches a value of $\sqrt{2/\pi k}$ as $R \to \infty$.

B. Multichannel *K*-matrix approach

For each energy degenerate open channel $\gamma_o E$, we define a wave function at an energy E using the basis set given by Eq. (5) in the form

$$|\Phi_{\gamma_o E}\rangle = |\gamma_o E\rangle + \sum_{\gamma}' d\varepsilon\, \mathcal{P}|\gamma\varepsilon\rangle \frac{\langle \gamma\varepsilon | K(E) | \gamma_o E\rangle}{E-\varepsilon}, \qquad (9)$$

where the sum $\Sigma' = (\Sigma + \int)$ includes the summation over all discrete components and the integration over the entire continua, and $\mathcal{P}$ denotes the principal part of the integral. For each basis set $|\gamma'\varepsilon'\rangle$, the condition

$$\langle \gamma'\varepsilon' | H-E | \Phi_{\gamma_o E}\rangle = 0 \qquad (10)$$

leads to a set of coupled integral equation for the K matrix, i.e.,

$$\langle \gamma'\varepsilon' | K(E) | \gamma_o E\rangle = \langle \gamma'\varepsilon' | V(E) | \gamma_o E\rangle$$
$$+ \sum_{\gamma}' d\varepsilon\, \mathcal{P}\langle \gamma'\varepsilon' | V(E) | \gamma\varepsilon\rangle$$
$$\times \frac{\langle \gamma\varepsilon | K(E) | \gamma_o E\rangle}{E-\varepsilon}. \qquad (11)$$

The energy-dependent V matrix, given by

$$\langle \gamma'\varepsilon' | V | \gamma\varepsilon\rangle \equiv \langle \gamma'\varepsilon' | H-E | \gamma\varepsilon\rangle - (\varepsilon-E)\delta_{\gamma'\gamma}\delta(\varepsilon-\varepsilon'), \qquad (12)$$

can be evaluated with the same numerical procedure employed in the BSCI calculation. The open-channel wave functions defined by Eq. (9) satisfy the same *orthogonality* condition obtained in the K-matrix approach by Moccia and co-workers [6], i.e.,

$$\langle \Phi_{\gamma'E'} | \Phi_{\gamma E}\rangle = \delta(E'-E)\left[\delta_{\gamma'\gamma} + \pi^2 \sum_{\gamma''} \langle \gamma''E | K(E) | \gamma'E\rangle\right.$$
$$\left. \times \langle \gamma''E | K(E) | \gamma E\rangle\right]. \qquad (13)$$

C. Eigenchannels

Following the same procedure employed by Starace [5], the eigenstate $|\Gamma E\rangle$ of the eigenchannel Γ at an energy E may be expressed as a linear combination of the open-channel wave functions according to Eq. (1). It can be shown readily that the eigenstate $|\Gamma E\rangle$ satisfies the usual *orthonormality* relation

$$\langle \Gamma' E' | \Gamma E \rangle = \delta_{\Gamma'\Gamma} \delta(E'-E) \tag{14}$$

if the transformation matrix $U_{\gamma_o \Gamma}(E)$ and the eigenphase shift η_Γ are obtained by diagonalizing the *on the energy shell K* matrix, i.e.,

$$\sum_\gamma \langle \gamma_o E | K(E) | \gamma E \rangle U_{\gamma\Gamma} = -\pi^{-1} \tan \eta_\Gamma U_{\gamma_o \Gamma}. \tag{15}$$

Similar to the increase of the scattering phase shift by a value of π across a resonance embedded in a single continuum, Hazi [9] simplified a more general expression derived by Macek [8], and showed that the sum of the eigenphase shift over all eigenchannels, i.e.,

$$\eta_{tot} = \sum \eta_\gamma, \tag{16}$$

also increases by a total of π as the energy increases across an isolated resonance. As a result, the total width of a resonance can be calculated readily from the energy variation of η_{tot}.

To calculate the partial and total photoionization cross sections, we shall first proceed to construct a state wave function $|\gamma E^-\rangle$, which satisfies the energy normalization according to

$$\langle \gamma' E'^- | \gamma E^- \rangle = \delta_{\gamma'\gamma} \delta(E'-E) \tag{17}$$

for each of the ionization channel. From Eq. (14), it can be shown immediately that the normalization condition [Eq. (16)] is satisfied if

$$|\gamma E^-\rangle = \sum_\Gamma |\Gamma E\rangle C_{\Gamma\gamma}, \tag{18}$$

where $C_{\Gamma\gamma} = e^{-i\eta_\Gamma} \tilde{U}_{\Gamma\gamma} e^{-i\delta_\gamma}$. The interchannel interactions between all open channels are included in the state function $|\gamma E^-\rangle$ in terms of $U_{\gamma_o\Gamma}$ and η_Γ. The channel function

$$\Psi_{\gamma E}(\vec{r}_1 \vec{s}_1, \ldots, \vec{r}_N \vec{s}_N) \equiv \langle \vec{r}_1 \vec{s}_1, \ldots, \vec{r}_N \vec{s}_N | \gamma E^- \rangle \tag{19}$$

contains outgoing spherical waves only in channel γ, and its asymptotic form is identical to Eq. (4.56) in Ref. [5].

D. Photoionization cross sections

The total photoionization cross section is given by the sum of the partial cross sections over all open channels, i.e.,

$$\sigma_{tot} = \sum_\gamma \sigma_\gamma. \tag{20}$$

The partial cross section in unit of a_0^2 for each open channel γ is given by

$$\sigma_\gamma = 4\pi^2 \alpha f_{\gamma I}, \tag{21}$$

where

$$f_{\gamma I}^{(L)}(E) = \frac{\Delta E}{3g_I} \sum_{\text{all } M's} \left| \langle \Psi_I | \sum \vec{r}_i | \gamma E^- \rangle \right|^2 \tag{22}$$

and

$$f_{\gamma I}^{(V)}(E) = \frac{4}{3g_I(\Delta E)} \sum_{\text{all } M's} \left| \langle \Psi_I | \sum \vec{\nabla}_i | \gamma E^- \rangle \right|^2 \tag{23}$$

are the *effective* oscillator strengths corresponding to *length* and *velocity* approximations, respectively. The excitation energy $\Delta E = E - E_I$ is given in Ry units and the degeneracy of the initial state I is given by $g_I = (2S_I+1)(2L_I+1)$. The wave function $|\Psi_I\rangle$ for the initial state I is calculated using the BSCI procedure.

III. NUMERICAL PROCEDURE

A. Discretized *K* matrix

The second term on the right-hand side of the *coupled integral equation* for the *K* matrix given by Eq. (11) can be reduced into a single discretized term $K^{(1)}$ if γ represents a closed channel, i.e.,

$$K^{(1)} = \sum_\gamma \sum_{I_\gamma} \langle \gamma' \varepsilon' | V(E) | \gamma \varepsilon_{I_\gamma} \rangle \frac{\langle \gamma \varepsilon_{I_\gamma} | K(E) | \gamma_o E \rangle}{E - \varepsilon_{I_\gamma}}, \tag{24}$$

where I_γ in Eq. (24) is the index for the discrete basis in channel γ. If γ represents an *open* channel, a contribution from a second discretized term $K^{(2)}$,

$$K^{(2)} = \sum_\gamma \sum_i \mathcal{P} \int_{\varepsilon_i}^{\varepsilon_{i+1}} d\varepsilon \langle \gamma' \varepsilon' | V(E) | \gamma \varepsilon \rangle \frac{\langle \gamma \varepsilon | K(E) | \gamma_o E \rangle}{E - \varepsilon}, \tag{25}$$

should be added. The *principal* part of the integral in Eq. (25) is evaluated only when E lies within the ith energy intervals between ε_i and ε_{i+1} for the *open* channel γ.

Alternatively, the term $K^{(1)}$ can be expressed as a matrix element of a product of three maticies $V(E)$, $X(E)$, and $K(E)$, i.e.,

$$K^{(1)} = \langle \gamma' \varepsilon' | V(E) X(E) K(E) | \gamma_o E \rangle, \tag{26}$$

where

$$\langle \gamma' \varepsilon_{\nu'} | X(E) | \gamma \varepsilon_\nu \rangle = \delta_{\gamma\gamma'} \delta_{\nu\nu'} \frac{1}{E - \varepsilon_\nu}. \tag{27}$$

More elaborate procedures are required to evaluate the principal value intergration in $K^{(2)}$. We will follow a procedure similar to the one employed by Moccia and co-workers [6]. Instead of starting from the usual Lagrange interpolation, the value of a function f at x may be interpolated using an alternative expression in terms of a polynomial

$$f(x) = \sum_{m'=1}^{N} \left(\sum_m \alpha_{mm'} f(x_m) \right) x^{m'-1}, \tag{28}$$

where m and m' are indices for a set of N grid points, and the expansion coefficients $\alpha_{mm'}$ are functions of the grid points. The matrices $\langle \gamma' \varepsilon' | V(E) | \gamma \varepsilon \rangle$ and $\langle \gamma \varepsilon | K(E) | \gamma_o E \rangle$ in Eq. (25) can be approximated as

$$\sum_{m'=1}^{N} \left(\sum_{m} \alpha_{mm'} \langle \gamma' \varepsilon' | V(E) | \gamma \varepsilon_m \rangle \right) \varepsilon^{m'-1} \quad (29)$$

and

$$\sum_{n'=1}^{N} \left(\sum_{n} \alpha_{nn'} \langle \gamma \varepsilon_n | K(E) | \gamma_o E \rangle \right) \varepsilon^{n'-1}, \quad (30)$$

respectively. Similar to the expression given in Eq. (26) for $K^{(1)}$, we can now express the term $K^{(2)}$ as a matrix element of a product of three matices, $V(E)$, $Y(E)$, and $K(E)$, i.e.,

$$K^{(2)} = \langle \gamma' \varepsilon' | V(E) Y(E) K(E) | \gamma_o E \rangle, \quad (31)$$

where

$$\langle \gamma' \varepsilon_m | Y(E) | \gamma \varepsilon_n \rangle = \delta_{\gamma \gamma'} \sum_{i} Y_{mn}^{(i)} \quad (32)$$

and

$$Y_{mn}^{(i)} = \sum_{m',n'=1}^{N} \alpha_{m\,m'} \alpha_{n\,n'} \int_{\varepsilon_i}^{\varepsilon_{i+1}} d\varepsilon \, \mathcal{P} \frac{\varepsilon^{m'+n'-2}}{E-\varepsilon}. \quad (33)$$

From Eqs. (24)–(26) and (31), the coupled intergral equations for the K matrix shown in Eq. (11) can now be written as a set of equations in terms of a *discretized K* matrix $K^d(E)$,

$$\langle \gamma' \varepsilon' | [1 - V(E)P(E)] K^d(E) | \gamma_o E \rangle = \langle \gamma' \varepsilon' | V(E) | \gamma_o E \rangle, \quad (34)$$

where $P(E)$ is a square matrix given by

$$P(E) = X(E) + Y(E). \quad (35)$$

Most of the off-diagonal elements of the $P(E)$ matrix equal zero, and its near diagonal structure was discussed in detail by Moccia and co-workers [6]. Finally, the K matrix, in terms of K^d, is evaluated numerically from

$$K^d(E) = \frac{1}{[1 - V(E)P(E)]} V(E). \quad (36)$$

B. Transition amplitude

For a two-electron atom or an alkaline-earth atom, similar to the the BSCI approach, Eqs. (22) and (23) can be written in a form which can be evaluated more conveniently after a straightforward application of the angular momentum algebra, i.e.,

$$f_{\gamma_o I}^{(L)}(E) = \delta_{S_{\gamma_o} S_I} \frac{(2L_{\gamma_o}+1)}{3} \Delta E |T_{\gamma_o I}^{(L)}(E)|^2 \quad (37)$$
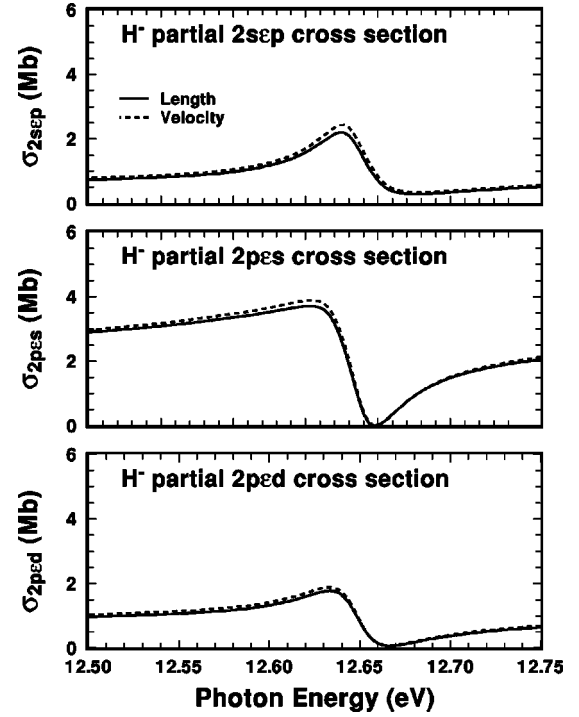

FIG. 1. Partial photodetachment cross sections near the $N=3$ threshold of H from the H$^-$ ground state.

and

$$f_{\gamma_o I}^{(V)}(E) = \delta_{S_{\gamma_o} S_I} \frac{4(2L_{\gamma_o}+1)}{3\Delta E} |T_{\gamma_o I}^{(V)}(E)|^2. \quad (38)$$

The total transition amplitude $T_{\gamma I}$ is given by

$$T_{\gamma I}(E) = \sum_{\Gamma \gamma_o} t_{\gamma_o I}(E) U_{\gamma_o \Gamma}(E) \cos \eta_\Gamma(E) C_{\Gamma \gamma}(E), \quad (39)$$

where

$$t_{\gamma_o I} = F_{\gamma_o E, I} + \sum_{\nu', \gamma \nu} F_{\gamma \nu', I} \langle \gamma \nu' | P | \gamma \nu \rangle \langle \gamma \nu | K | \gamma_o E \rangle. \quad (40)$$

The same expression given by Eq. (43) in Ref. [2] can then be applied to evaluate the transition matrix $F_{\gamma \nu, I}$.

IV. RESULTS AND DISCUSSIONS

Figure 1 presents the partial photodetachment cross sections from the ground state of H$^-$ into the $2s\varepsilon p$, $2p\varepsilon s$, and $2p\varepsilon d$ channels near the resonance below the $N=3$ threshold of H. The partial photodetachment cross sections into the $1s\varepsilon p$ ionization channel shown in Fig. 2 are similar in magnitude to those into the individual $N=2$ ionization channels. The total $N=2$ partial cross sections and the total H$^-$ photodetachment cross sections are also shown in Fig. 2. Our calculated spectrum is in close agreement with the earlier experimental and theoretical results (e.g., see Refs. [10,11]). Our calculated width of 2.41×10^{-3} Ry is also in close
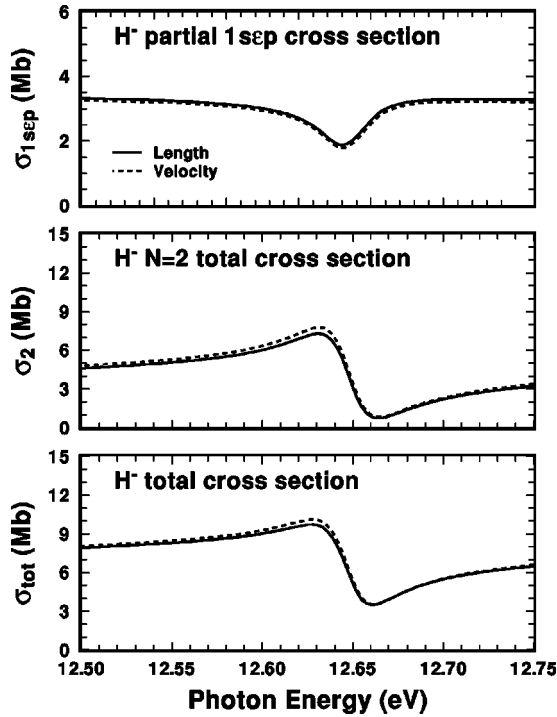
FIG. 2. Partial and total photodetachment cross sections near the $N=3$ threshold of H from the H$^-$ ground state.

agreement with earlier experimental and theoretical results [10–13]. The agreement between our length and velocity results are very good as shown.

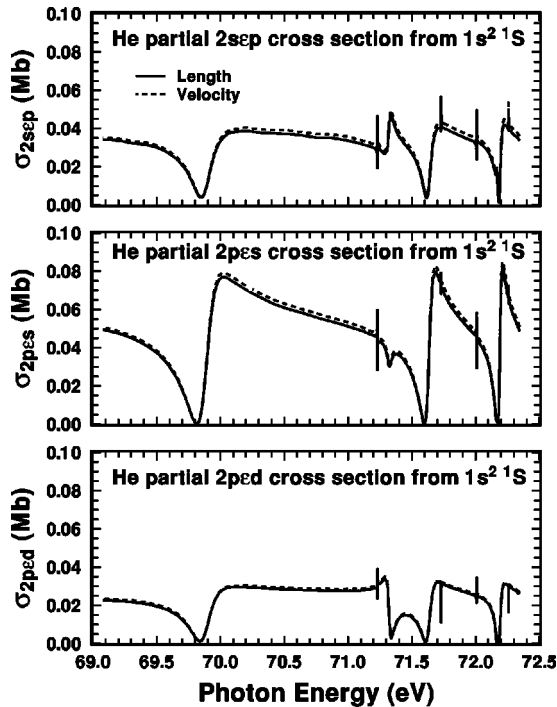As a second test, we have applied the BSK approach to the He photoionization above the $N=2$ threshold. Our cal-

TABLE I. Comparison of the widths (in $a[\mu]=a\times10^{\mu}$ eV) from the BSK calculation for a few selected resonances converging to the $N=3$ threshold of He$^+$ with theoretical data from Moccia and co-workers [6] and the complex rotational method of Ho [17]. The resonances are labeled according to the notation introduced by Lin [18].

State	Present	Ref. [17]	Ref. [6]
1_3^+	$1.96[-1]$	$1.80[-1]$	$1.84[-1]$
2_4^-	$9.30[-4]$	$9.28[-4]$	$8.75[-4]$
-1_3^+	$3.76[-2]$	$3.97[-2]$	$3.74[-2]$
1_4^+	$7.97[-2]$	$7.89[-2]$	$8.18[-2]$
0_4^-	$6.60[-4]$	$6.16[-4]$	$5.84[-4]$
2_5^-	$5.58[-4]$	$5.90[-4]$	$5.95[-4]$
-1_4^+	$1.31[-2]$	$1.41[-2]$	$1.82[-2]$
1_5^+	$3.16[-2]$	$3.53[-2]$	$2.91[-2]$
0_5^-	$2.95[-4]$	$2.91[-4]$	$2.75[-4]$

culated partial photoionization cross sections into the $2s\varepsilon p$, $2p\varepsilon s$, and $2p\varepsilon d$ ionization channels are shown in Fig. (3). Again, our results (including the partial cross sections into the $1s\varepsilon p$ ionization channel not shown here) are in close agreement with the earlier results by Moccia and co-workers [6] and Zhou and Lin [14]. The calculated spectrum also agree well with the observed spectra [15,16]. The widths of the resonances are determined from the energy variation of the sum of the eigenphase shifts as discussed in Sec. II C. In Table I, we compare our calculated widths for a few selected resonances with the earlier theoretical results by Moccia co-workers [6] and the complex rotational calculation by Ho [17]. The agreement is in general very good. More detailed reviews of He photoionization above the $N=2$ threshold were already given in Refs. [6] and [14].
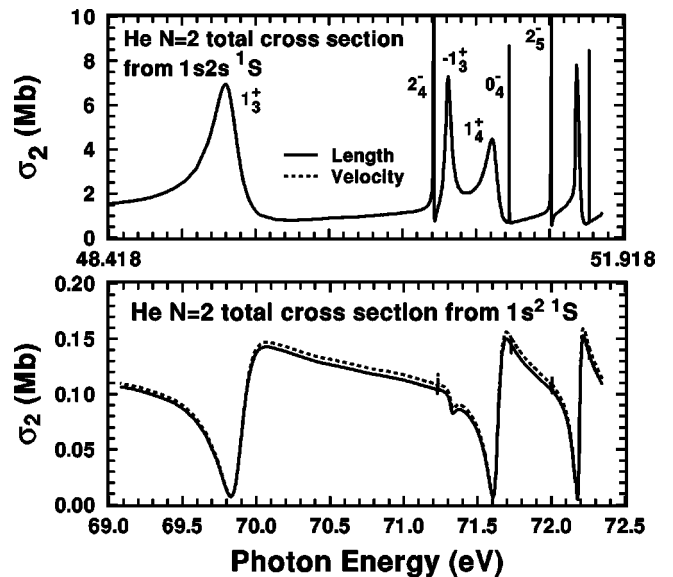

FIG. 3. Partial photoionization cross sections converging to the $N=3$ threshold of He$^+$ from the He ground state.

FIG. 4. Comparison of doubly excited spectra converging to the $N=3$ threshold of He$^+$ between photoionization from the $1s2s\ ^1S$ metastable state and $1s^2\ ^1S$ ground states.
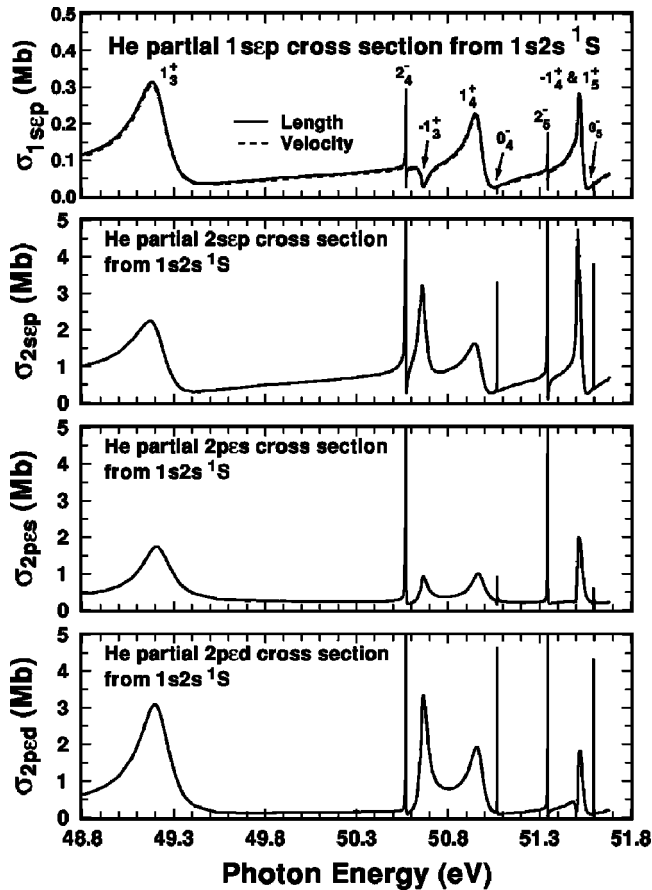
FIG. 5. Partial photoionization cross sections converging to the $N=3$ threshold of He$^+$ from the He $1s2s\,^1S$ metastable state.

FIG. 6. Separation between He-1_4^+ and 1_5^+ resonances seen in the He$1s2s\,^1S$ partial $2p\varepsilon d$ spectrum.

photoionization, is its ability to extend to photoionization from bound excited states with little additional effort. As a by-product of our ground-state calculation, we have carried out a four-channel photoionization calculation between the $N=2$ and 3 thresholds of He$^+$ from the $1s2s\,^1S$ metastable state. Figure 4 compares the total $N=2$ cross sections from the $1s2s\,^1S$ state to the ones from the He ground state. Clearly, the resonance profiles for the narrow resonances are far more prominent than those seen in the ground-state spectrum. The substantially larger cross sections from the metastable state should also help the experimental measurement. Detailed partial photoionization cross sections are presented in Fig. 5. Unlike photoionization from the ground state, the partial cross sections going into the $N=2$ channels are substantially larger than the one going into the $N=1$ channel. We also note that some of the resonancs which have been identified theoretically are difficult to resolve in the photoionization spectrum. One such example is the two neighboring -1_4^+ and 1_5^+ resonances. Only on an enlarged scale and only in the $2p\varepsilon d$ spectrum shown in Fig. 6 can these two resonances be separated. Our results also confirm quantitatively the earlier *hyperspherical close-coupling* results by Zhou and Lin [14].

In conclusion, we have presented a detailed theoretical procedure using the BSK approach for atomic photoionization from two-electron and divalent (e.g., alkaline-earth) atoms. We have also demonstrated its effectiveness as a viable quantitative approach. Finally, it is hoped that our theoretical result for the photoionization from excited state may lead to new experimental advancement.

The main difficuty for a detailed comparison of the narrow resonances between the experiment and theory is due to the *windowlike* nature of the spectrum. The cross sections in the vicinity of the resonances are also relatively small due to the simultaneous excitation of two electrons. In spite of the substantial recent advancement in vacuum ultraviolet light source, the energy resolution is not sufficient to resolve most of the narrow structures which are barely visible in the calculated spectra. As we, and a few others, have suggested in recent years, an alternative and perhaps more precise characterization of the doubly excited resonances may be obtained using spectra from the bound excited states [1,14,19,20]. A new experimental technique has indeed been developed to measure the photoionization from bound excited states with success. In fact, one of our recent works on photoionization from bound excited states to nonresonant region [21] has already been confirmed by such an experiment [22].

Similar to the *R*-matrix or close-coupling approach [23,24], one of the key advantages enjoyed by a *B*-spline-based calculational approach, when it is applied to atomic
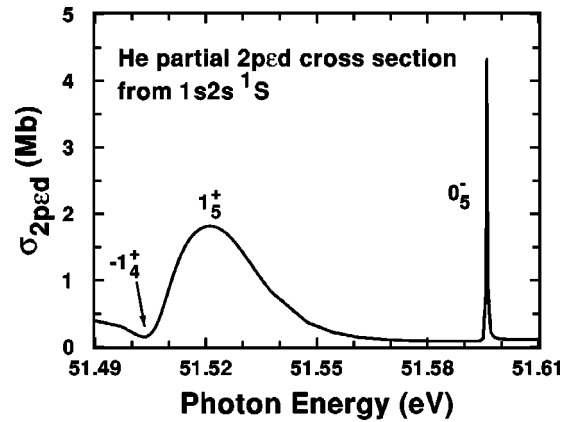
[1] T.N. Chang and X. Tang, Phys. Rev. A **44**, 232 (1991).

[2] T.N. Chang, in *Many-Body Theory of Atomic Structure and Photoionization*, edited by T.N. Chang (World Scientific, Singapore, 1993), p. 213.

[3] T.K. Fang and T.N. Chang, Phys. Rev. A **56**, 1650 (1997); T.N. Chang, T.K. Fang, Y.S. Kim, and B.I. Nam, J. Korean, J. Korean Phys. Soc. **32**, 200 (1998).

[4] T.K. Fang, B.I. Nam, Y.S. Kim, and T.N. Chang, Phys. Rev. A

55, 433 (1997); T.N. Chang and X. Tang, **46**, R2209 (1992).

[5] A.F. Starace, in *Handbuch der Physik*, edited by W. Mehlhorn (Springer, Berlin, 1980), Vol. 31, p. 1.

[6] R. Moccia and P. Spizzo, Phys. Rev. A **43**, 2199 (1991); V. Carravetta, P. Spizzo, and R. Moccia, in *Many-Body Theory of Atomic Structure and Photoionization* (Ref. [2]), p. 175.

[7] T.N. Chang and Y.S. Kim, Phys. Rev. A **34**, 2609 (1986).

[8] J. Macek, Phys. Rev. A **2**, 1101 (1970).

[9] A.U. Hazi, Phys. Rev. A **19**, 920 (1979).

[10] J.Z. Tang, Y. Wakabayashi, M. Matsuzawa, S. Watanabe, and I. Shimamura, Phys. Rev. A **49**, 1021 (1994).

[11] M. Halka, H.C. Bryant, E.P. Mackerrow, W. Miller, A.H. Mohagheghi, C.Y. Tang, S. Cohen, J.B. Donahue, A. Hsu, C. Quick, J. Tiee, and K. Rosza, Phys. Rev. A **44**, 2199 (1991).

[12] Y.K. Ho, Phys. Rev. A **45**, 148 (1992).

[13] H.R. Sadeghpour, C.H. Greene, and M. Cavagnero, Phys. Rev. A **45**, 1587 (1992).

[14] B. Zhou and C.D. Lin, Phys. Rev. A **49**, 1057 (1994).

[15] D.W. Lindle, T.A. Ferrett, P.A. Heimann, and D.A. Shirley, Phys. Rev. A **36**, 2112 (1987); K. Schulz, G. Kaindl, M.

Domke, J.D. Bozek, P.A. Heimann, A.S. Schlachter, and J.M. Rost, Phys. Rev. Lett. **77**, 3086 (1996).

[16] J.A.R. Samson, Z.X. He, L. Yin, and G.N. Haddad, J. Phys. B **27**, 887 (1994); G.V. Marr and J.B. West, At. Data Nucl. Data Tables **18**, 497 (1976).

[17] Y.K. Ho, Phys. Rev. A **44**, 4154 (1991).

[18] C.D. Lin, Adv. At. Mol. Phys. **22**, 77 (1986).

[19] T.N. Chang, L. Zhu, Phys. Rev. A **48**, R1725 (1993).

[20] J.Z. Tang and I. Shimamura, Phys. Rev. A **50**, 1321 (1994); B. Zhou, C.D. Lin, J.Z. Tang, S. Watanabe, and M. Matsuzawa, J. Phys. B **26**, L337 (1993).

[21] T.N. Chang and T.K. Fang, Phys. Rev. A **52**, 2638 (1995).

[22] M. Gisselbrecht, D. Descamps, C. Lynga, A. L'Huillier, C.-G. Wahlstrom, and M. Meyer, Phys. Rev. Lett. **82**, 4607 (1999).

[23] P. G. Burke, in *Many-Body Theory of Atomic Structure and Photoionization* (Ref. [2]) p. 47; L. Quigley and K. Berrington, J. Phys. B **29**, 4529 (1996); M.A. Hayes and M.P. Scott, *ibid.* **21**, 1499 (1988).

[24] J.A. Fernley, K.T. Taylor, and M.J. Seaton, J. Phys. B **20**, 6457 (1987).